Journal of Applied Electrochemistry **32**: 1363–1370, 2002.

Electrochemical behaviour of low carbon steel in concentrated carbonate chloride brines

F.M. AL-KHARAFI*, B.G. ATEYA and R.M. ABDALLAH
Chemistry Department, Faculty of Science, Kuwait University, PO Box 5969, Safat, 13060 Kuwait
*(*author for correspondence, e-mail: faiza@kuc01.kuniv.edu.kw)*

Received 24 March 2002; accepted in revised form 6 September 2002

Key words: brine, carbonate, chloride, green rust, iron, passivity, pitting

Abstract

The polarization curves of low carbon steel in deaerated carbonate bicarbonate buffers (pH 10.3) show three distinct regions: (a) an active region characterized by a Tafel slope of 125 ± 5 mV which is independent of the chloride concentration, (b) a gradual active to passive transition, and (c) a broad passive region. The addition of NaCl has a stronger effect on the passive than on the active region. For NaCl concentrations of 0.1 to 2 M, NaCl has only a small promoting effect (a reaction order of 0.1) on the anodic dissolution of the steel in the active region. Measurements of electrochemical impedance under free corrosion conditions confirm the above findings. The results are explained in terms of the more favourable formation of an iron hydroxy-carbonate complex (called green rust carbonate) than the formation of the corresponding green rust chloride complex. Passivity is attributed to the formation of a protective film containing both FeOOH and Fe_2O_3. It deteriorates with increasing chloride concentration and potential and improves with increase of buffer concentration. Evidence is also presented for metastable pitting, particularly in the presence of the lower chloride concentration, for example, 0.1, 0.2 and 0.5 M NaCl.

1. Introduction

The electrochemical behaviour of low carbon steel in concentrated carbonate–chloride brines is of particular significance to the corrosion problems encountered in drilling for the production of oil and gas [1–4] and for the recovery of geothermal energy. Many of the components of drilling gears, down hole tubulars and production vessels are fabricated from low carbon steel. The service environment of these components is geothermal brine which contains significant concentrations of CO_2, H_2S and chloride ions at fairly high temperatures. While CO_2 leads to extensive pitting of iron and various other steels [3, 5], H_2S (particularly in sour wells) leads to catastrophic failures caused by stress corrosion cracking and hydrogen embrittlement [6]. These are problems of particular concern to the countries of the Gulf region which produce a substantial share of world oil and natural gas. Among the more common techniques to control CO_2 and H_2S corrosion of drilling equipment is the injection of caustic soda or calcium hydroxide in the wells to raise the pH above 9.5 [1]. This neutralizes the acids and lowers their levels in the brine by facilitating the precipitation of iron sulfide and iron carbonate upon injection of the H_2S and CO_2 scavengers [1]. The subject is also important in connection with the corrosion of steel rebars in concrete [7], the corrosion of steel packages proposed for geological disposal of high level nuclear wastes [8] and the stress corrosion cracking of gas and oil pipelines [9]. In view of the importance of the Fe/carbonate system, it has been attracting renewed interest, where various techniques have been employed to characterize the reaction products and to unravel the reaction mechanism [10–21]. The presence of chloride ions is bound to affect the behaviour of the metal in the carbonate medium.

In this paper we present the results of a systematic study of the electrochemical behaviour of iron in carbonate–chloride media of various concentrations. This been extensively studied in strongly acidic media and to a much lesser extent in the slightly acidic or alkaline media [22–26].

2. Experimental details

The low carbon steel was obtained from Goodfellow, in the form of rods having the following composition: 0.2% C, 0.94% Mn, 0.31% Si and normal traces of Ni, Cr and Mo. The rod was mounted in a glass tube of appropriate diameter using epoxy resin leaving a specified circular surface area (0.20 cm^2) to contact the electrolyte. The working electrode was polished using successive grades of SiC down to 1200 grit, followed by

0.3 and 0.05 μm alumina to give a mirror like finish. The test solutions were prepared from deionized water and AnalaR grade chemicals. They were de-aerated by bubbling Ar for 25 min before testing. An airtight three electrode polarization cell was used for all measurements. An Ag/AgCl electrode ($E = 0.197$ V vs SHE) was used as reference and a platinum wire was used as the counter electrode. The polarization measurements were performed using an EG&G (PAR model 273A) corrosion measurement system. The electrode was immersed in the electrolyte and left for about 15 min to attain a steady free corrosion potential before performing potentiodynamic or impedance measurements. Unless otherwise indicated, potentiodynamic measurements were performed at a potential scanning rate of 1 mV s^{-1} starting from cathodic going into anodic potentials. The impedance measurements were performed under open circuit conditions using an IM5D impedance analyser (Zahner Electrik GmbH, Kronach, Germany). The temperature of the test electrolyte was controlled by immersing the cell in a water thermostat adjusted at 30 ± 0.1 °C.

3. Experimental results

3.1. *Polarization curves*

Figure 1 shows the polarization curves obtained in the blank electrolyte and after addition of 0.1 M or 0.2 M NaCl. In all electrolytes there is a major anodic peak (peak A) followed by smaller peaks and a gradual active to passive transition indicated by more than one order of magnitude decrease in the current. Similar peaks have been observed by many workers in various media [10, 12, 14, 23 and 25]. Peak A represents active dissolution of the metal and is accompanied with a Tafel region. The anodic Tafel slopes were calculated from the linear regions in the ascending part of peak A at various chloride concentrations. The Tafel slope was found to be a fairly constant value (125 ± 5 mV) independent of the concentration of NaCl. These values compare favourably with values of 115 ± 10 mV [23] and 120 mV [22] obtained from transient measurements at 25 °C. A Tafel slope of about 120 mV at room temperature is often obtained for one electron transfer reactions under activation control.

3.2. *Passive region*

Beyond the peak potential, the current falls gradually with potential over a region that has been associated with passive layer formation [23]. This gradual potential dependent approach to passivity in the blank electrolyte is quite unlike that of iron in other media, e.g. sodium sulphate or sulfuric acid, where a well defined passivation potential is observed. It is suggestive of a potential dependent passivation process. In the blank electrolyte, a broad passive region is observed, extending for about 1 V from −200 to +800 mV vs (Ag/AgCl) over which the passive current is about 10 μA cm^{-2}. This passive behaviour has been documented by previous workers [10, 12, 14, 17] and is attributed to the formation of reaction products which protect the surface. These protective films had been characterized using (SERS) surface enhanced Raman spectroscopy [10, 13, 15], conversion electron Mössbauer spectroscopy [17, 27–31], XRD [11, 12, 17, 18, 27–31], XPS [11, 21], EDX [12], electrochemical impedance spectroscopy [12, 14] and infra red spectroscopy [12]. The composition of the reaction product is believed to be dependent on temperature, potential and pH [12, 13]. Various workers have presented evidence which suggests that the film contains Fe_2O_3 [18, 21], Fe_3O_4 [10, 18], $Fe\,CO_3 \cdot H_2O$

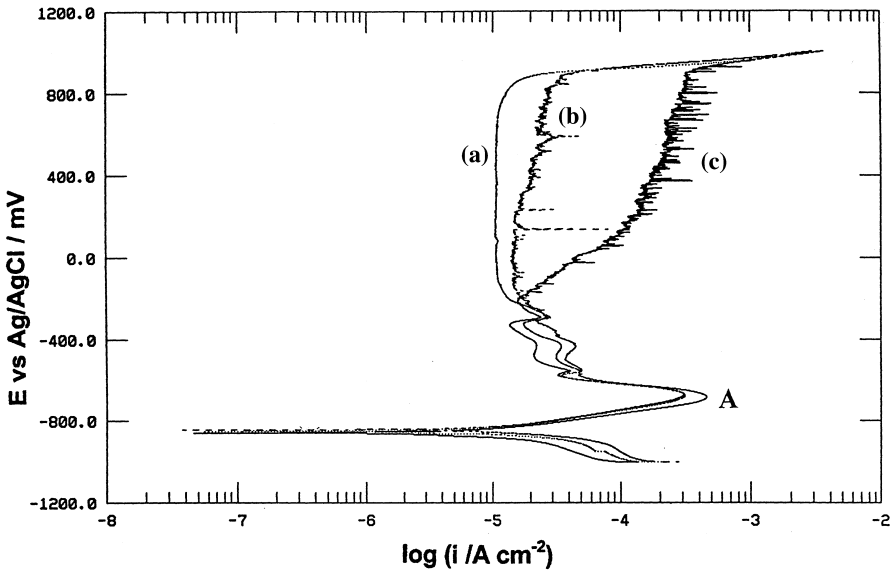

Fig. 1. Polarization curves of low carbon steel in (a) 0.5 M CO_3^{2-} + 0.5 M HCO_3^- buffer, (b) buffer +0.1 M Cl^- ions and (c) buffer +0.2 M Cl^- ions.

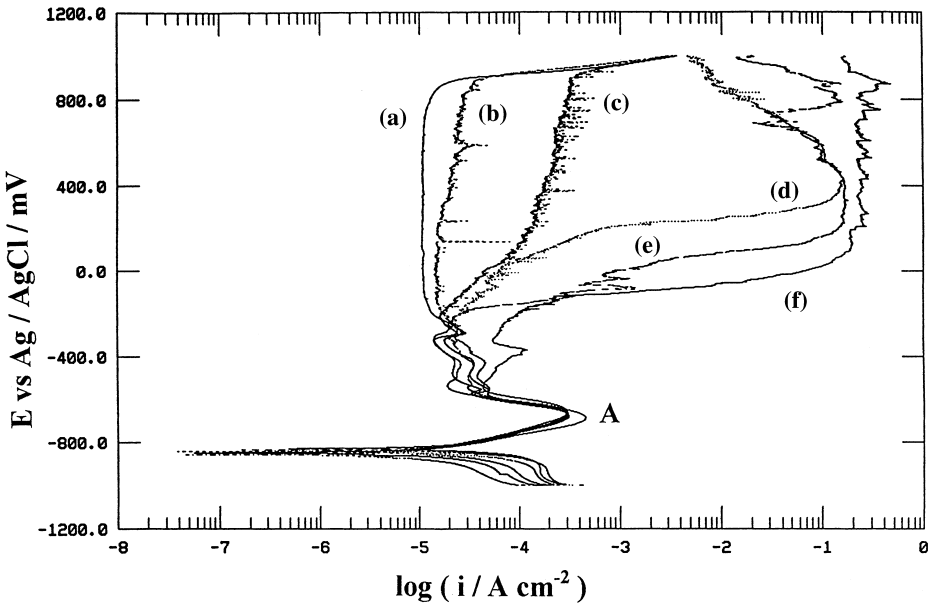

Fig. 2. Comparison of polarization curves of low carbon steel in 0.5 M carbonate–0.5 M bicarbonate buffer in the presence of small and large concentrations of chloride ions, (a, b, c, d, e and f) correspond to 0, 0.1, 0.2, 0.5, 1 and 2 M chloride, respectively.

[10, 12, 21], FeOOH [10, 17], or green rust [12, 17, 27–31] which is a hydroxy complex involving both ferrous and ferric iron in addition to an anion, e.g. carbonate [28–30], sulfate [29] or chloride [27, 31].

3.3. *Chloride and buffer concentrations*

The presence of 0.1 M NaCl has a clear effect on the current in the passive region, Figure 1. The passive current is greater than that in the blank electrolyte and increases slowly, but gradually, with the increase in potential in the noble direction. More importantly, we observe frequent current spikes throughout the passive region and no discernible phenomenological pitting potential. We see a large number of small current spikes, of an amplitude of the order of few μA cm^{-2}, two spikes of about 15 μA cm^{-2} and one large spike of an amplitude of about 65 μA cm^{-2}. This is characteristic of metastable pitting, which often takes place at potentials less noble than the (phenomenological) measured pitting potential [32–41] and is associated with the formation of small (μm) metastable pits which quickly repassivate. Clearly, in this case (0.1 M NaCl), the average amplitude and frequency of the current spikes is determined by the large number of small spikes. In view of this, it can be concluded that in the presence of 0.1 M NaCl, only metastable pitting is possible over a range of potential of about 1 V.

As the chloride concentration increases to 0.2 M, Figure 1, a more pronounced increase in the current is observed in the passive region with increase in potential in the noble direction, starting at about −0.2 V vs Ag/AgCl. A similar phenomenon has also been reported for iron in an acidic medium [35]. Current spikes which have a much larger amplitude than those observed in the 0.1 M chloride also occur. A similar behaviour is also observed in the 0.5 M Cl^- medium, as shown in Figure 2, from −0.2 to +0.1 V vs Ag/AgCl before the sharp increase in current with potential. Figure 2 compares the polarization curves obtained in the presence of 0.1, 0.2, 0.5, 1 and 2 M NaCl dissolved in the carbonate–bicarbonate buffer. At concentrations of NaCl $\geqslant$ 0.5 M, dramatic increases of current are seen at the pitting potential, E_p while much smaller increases occur in the active region (see below) and only negligible changes are observed in the free corrosion potential. The value of E_p is taken at the point of sharp increase in current at a certain chloride concentration. For the case of 0.2 M Cl^-, it is taken at the intersection of the line representing the passive current with the descending part of the small peak immediately preceding it. The results of Figure 2 reveal that E_p becomes progressively less noble with increase in chloride concentration. Figure 3 shows the dependence of the pitting potential on the concentration of chloride ions in a buffer medium composed of 0.5 M CO_3^{2-} + 0.5 HCO_3^-, see (Figure 2). The plot gives a straight line with a slope of −170 mV for chloride concentrations up to 2 M. Similar relations

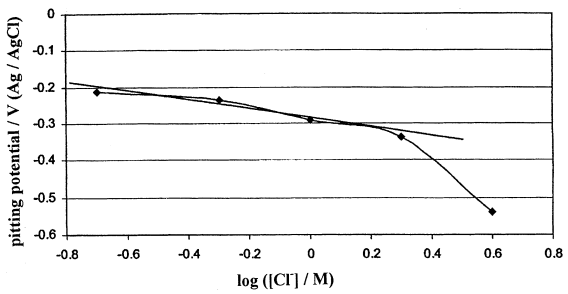

Fig. 3. Effect of concentration of NaCl on the pitting potential of low carbon steel in a buffer of 0.5 M CO_3^{2-} + 0.5 M HCO_3^-.

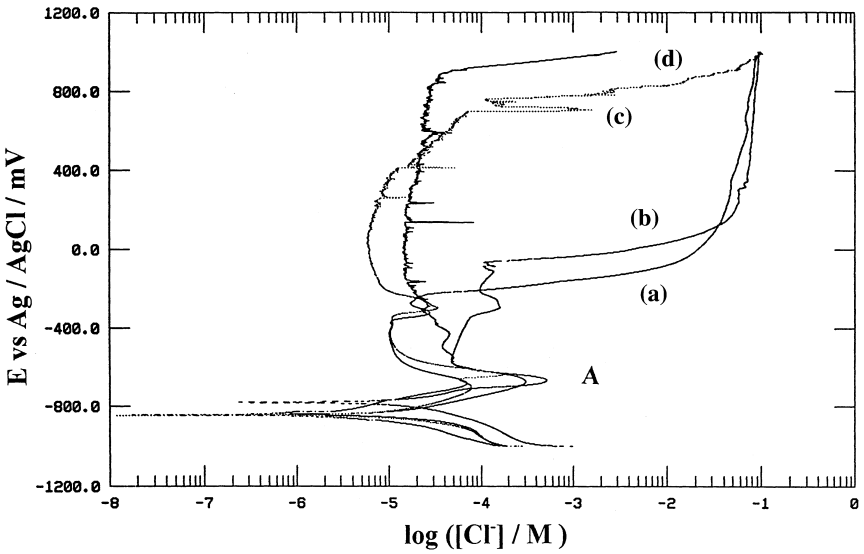

Fig. 4. Effect of concentration of CO_3^{2-} + HCO_3^- buffer on the polarization curves of the low carbon steel in presence of 0.1 M NaCl, (a, b, c and d) correspond to 0.1, 0.25, 0.5 and 1 M of each of carbonate and bicarbonate, respectively.

were reported for other metals and alloys [34]. Over this range of chloride concentrations, the pitting potential can be correlated to the concentration of the chloride ions using the equation:

$$E_p = -0.31 - 0.170 \log[Cl^-] \text{ V vs Ag/AgCl} \quad (1)$$

This value of slope (−0.170 V) can be compared with values ranging from 0.06 to 0.2 V reported for iron under various conditions [34]. For the case of the 4 M NaCl, the pitting potential is considerably less noble than the prediction of Equation 1. These values of pitting potentrials were measured at a potential scanning rate of 1 mV s^{-1} which is common practice. However, it is shown later (cf. Figure 6) that an order of magnitude decrease in the scanning rate does not significantly change the measured pitting potential.

Figure 4 shows the effect of concentration of the carbonate–bicarbonate buffer on the polarization curves obtained in the presence of 0.1 M NaCl. A decrease in the concentration of the buffer (CO_3^{2-} + HCO_3^-) results in a higher susceptibility to pitting as judged from the appearance of a more defined pitting potential at progressively less noble potentials. For instance while the pitting potential was about −250 mV vs Ag/AgCl in a buffer medium composed of 0.1 M CO_3^{2-} + 0.1 M HCO_3^-, it was about −70 mV vs Ag/AgCl in 0.25 M CO_3^{2-} + 0.25 M HCO_3^-, and no discernible pitting potential could be determined in the 0.5 M CO_3^{2-} + 0.5 M HCO_3^- or in the 1 M buffer. This can be understood on the basis of the increase in the concentration of the passivating carbonate and bicarbonate ions at the same concentration of the aggressive chloride ions. A similar effect has been reported for the borate buffer on the susceptibility of pitting of iron at pH 10.5 [42].

3.4. *Reaction order*

Although the concentration of NaCl has a strong effect on the behaviour of the steel in the passive region, its effect in the active (Tafel + peak A) region is only mild, (Figure 2). For a quantitative analysis of this effect, Figure 5 shows a logarithmic plot between the currents in the Tafel region and at peak A against the concentration of NaCl. Both sets of data give straight lines, with slopes of 0.1 over the concentration range 0.1 to 2 M, that is,

$$\frac{d \ln i}{d \ln[Cl^-]} \approx 0.1 \quad (2)$$

This very small reaction order indicates that the concentration of NaCl (from 0.1 to 2 M) has only a modest promoting effect on the rate of iron dissolution in the active region in the present medium (0.5 M CO_3^{2-} + 0.5 M HCO_3^-, pH ~10.3). The literature appears to have no references to similar measurements in this medium or pH to which we can compare this value. It is much smaller than the values of 0.5 (obtained at pH

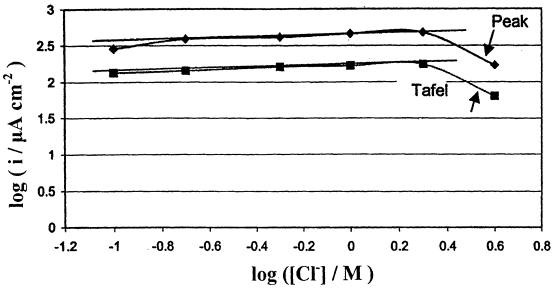

Fig. 5. Logarithmic plot of current in the active region against concentration of NaCl in the 0.5 M buffer medium.

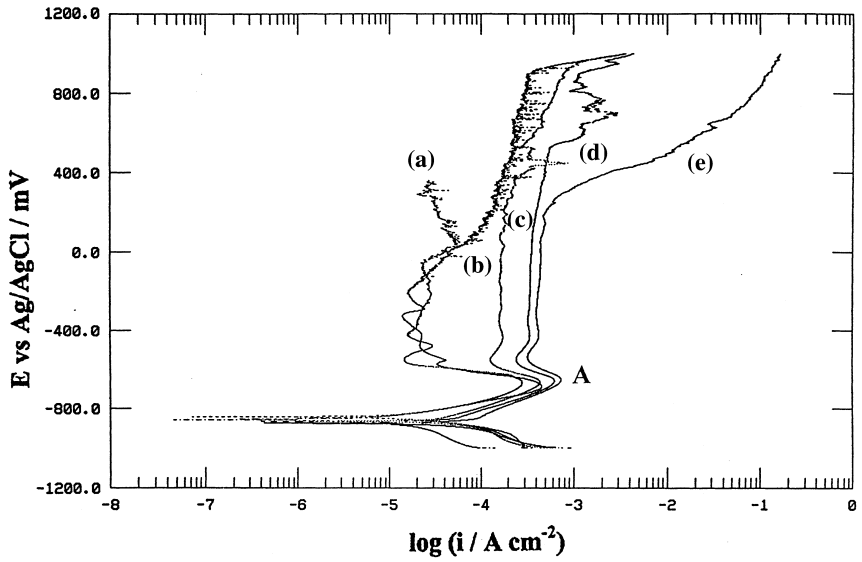

Fig. 6. Effect of potential scanning rate on the polarization curve of low carbon steel in a buffer solution of 0.5 M CO_3^{2-} + 0.5 M HCO_3^- in presence of 0.2 M NaCl, (a, b, c, d and e) correspond to 0.1, 1, 5, 10, and 20 mV s^{-1}, respectively.

of 0–1.8) and of 1.1 obtained in 4.5 M H^+ [43]. In the 4 M medium, the currents in both the Tafel region and at the peak are lower than the predictions of the straight-line relations. Another unusual effect of the 4 M chloride on the pitting potential is shown in Figure 3. The chloride ions at 4 M NaCl exhibit a different behaviour than that at lower concentrations. This is an interesting finding that ought to be pursued and analyzed. It was not possible to do measurements at higher concentrations of chloride ions because of the solubility limitation of NaCl in this medium at 30 °C. The exact mechanisms behind the effects of the 4 M chloride solution on the reaction order and on the pitting potential are yet to be determined.

3.5. *Scanning rate*

To further explore the effect of chloride ions, the polarization curves were measured at various potential scanning rates, in the presence of 0.2 M NaCl. Figure 6 shows the results obtained at scanning rates of 0.1, 1, 5, 10 and 20 mV s^{-1}. Clearly the scanning rate has a more pronounced effect on the current in the passive than in the active region. Figure 7 shows a logarithmic plot between the peak current and the voltage scanning rate. The results give a straight line with a slope of 0.2. Had a diffusional process in the aqueous phase supported the electrochemical reaction (producing the Tafel region and the active peak), the plot in Figure 7 would show a slope of 0.5 [44]. Combined with the very low value of reaction order (see above), this evidence indicates that chloride ions do not have a significant effect on the electrochemical behaviour of the low carbon steel in the active region.

An increase in the scanning rate increases the passive current significantly. This may be caused by an increasing in the nonfaradaic current which charges the double

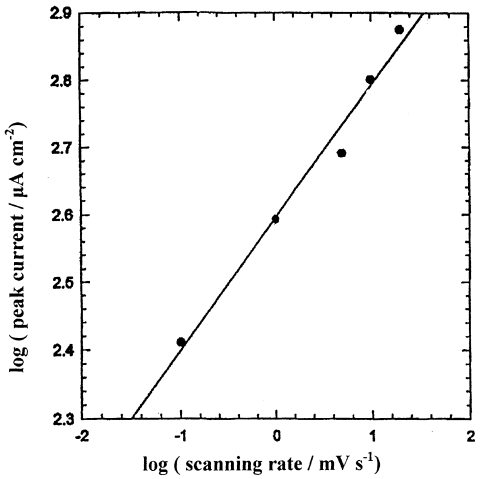

Fig. 7. Effect of the voltage scanning rate on peak current in a buffer solution of 0.5 M CO_3^{2-} + 0.5 M HCO_3^- in the presence of 0.2 M NaCl.

layer and/or an increase in the faradaic current supported by dissolution through the passive film. A simple calculation reveals that the charging current remains negligible compared to the measured current under all conditions of Figure 6, see (Appendix 1). On the other hand, the increase in the scanning rate results in a less protective passive layer by virtue of the fact that the electrode stays a much shorter period under a certain potential in the passive region.

3.6. *Electrochemical impedance*

The electrochemical impedance of the steel–electrolyte interface was measured under open circuit conditions in a buffer electrolyte (0.5 M CO_3^- + 0.5 M HCO_3^-) in the presence of 0, 0.1, 0.2, 0.5, 1and 2 M Cl^- ions. Figure 8 shows a collective Bode plot for these electrolytes. These

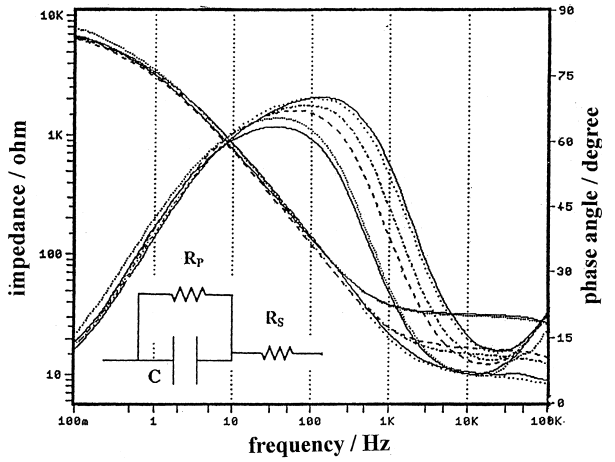

Fig. 8. Bode plots for low carbon steel, under open circuit potential, in presence of various concentrations of chloride ions: (——), (· · ·), (- - - -), (·-·-·-), (· · ·) and (——) for 0, 0.1, 0.2, 0.5, 1.0 and 2.0 M chloride, respectively.

curves can be analyzed in the light of the simple model of an RC line composed of an ideally polarizable electrode with a capacity C in series with the resistance of the electrolyte R_s, (inset in Figure 8). The Bode plot for this idealized system gives a straight line with a slope of -1 in the region of intermediate frequencies. The slope of the linear part in the region of intermediate frequencies in Figure 8 is about -0.8 which is taken as a reasonable approximation of the model predictions, particularly that we are using the impedance technique as a basis for a comparative study to show the effect of chloride ions. At the high frequency limit, the impedance Z approaches the solution resistance R_s, which varies from about 10 to 30 Ω with the concentration of chloride ions. On the other hand, at the low frequency limit, the impedance, Z approaches the sum of $R_s + R_p$ (far left of Figure 8), which is approximately equal to R_p by virtue of the fact that $R_s \ll Z$. At this limit, all the curves form a narrow band, indicating no significant effect of chloride ions on the impedance of the interface under free corrosion conditions in this medium. However, the chloride ions have a stronger effect on the maximum phase angle and hence on the double layer capacity of the interface. This point was not pursued further since it did not seem to have a significant effect on the polarization resistance and hence on the rate of corrosion.

4. Discussion

The active region in the polarization curve extends from the free corrosion potential (equivalent to about 0.550 V vs SHE) to the peak potential (equivalent to -0.480 V vs SHE). There are many electrochemical reactions that can support the anodic current in this region. Rafait and Genin et al. [27, 28] have computed extensive Pourbaix diagrams for iron in similar media. We present below only some of the electrochemical reactions which they considered and calculate their equilibrium potentials in the present medium (0.5 M CO_3^{2-} + 0.5 M HCO_3^-; pH 10.3):

$$Fe + 2H_2O = Fe(OH)_2 + 2H^+ + 2e^- \quad (3)$$

$$E = -0.0633 - 0.059\ pH$$
$$= -0.671\ V\ vs\ SHE$$

$$6Fe(OH)_2 + CO_3^{2-} + 2H_2O = Fe_6(OH)_{12}CO_3 \cdot 2H_2O + 2e^- \quad (4)$$

$$E = -0.63 - 0.0295 \log [CO_3^{2-}]$$
$$= -0.62\ V\ vs\ SHE$$

$$6Fe(OH)_2 + HCO_3^- + 2H_2O = Fe_6(OH)_{12}CO_3 \cdot 2H_2O + H^+ + 2e^- \quad (5)$$

$$E = -0.32 - 0.02 \log[HCO_3^-] - 0.0295\ pH$$
$$= -0.618\ V\ vs\ SHE$$

$$3Fe(OH)_2 = Fe(OH)_2 \cdot 2FeOOH + 2H^+ + 2e^- \quad (6)$$

$$E = 0.0615 - 0.059\ pH$$
$$= -0.546\ V\ vs\ SHE$$

$$4Fe(OH)_2 + Cl^- + nH_2O = Fe_4(OH)_8Cl \cdot nH_2O + e^- \quad (7)$$

$$E = -0.562 - 0.059 \log [Cl^-]$$
$$= -0.503\ V\ vs\ SHE\ for\ 0.1\ N\ NaCl$$
$$= -0.597\ V\ vs\ SHE\ for\ 4\ N\ NaCl$$

$$Fe_6(OH)_{12}CO_3 \cdot 2H_2O = 6\alpha - FeOOH + 2H_2O + CO_3^{2-} + 6H^+ + 4e^- \quad (8)$$

$$E = 0.41 + 0.0148 \log [CO_3^{2-}] - 0.0887\ pH$$
$$= -0.508\ V\ vs\ SHE$$

$$Fe_6(OH)_{12}CO_3 \cdot 2H_2O = 6\alpha - FeOOH + 2H_2O + HCO_3^- + 5H^+ + 4e^- \quad (9)$$

$$E = 0.26 + 0.0148 \log [HCO_3^-] - 0.0739\ pH$$
$$= -0.506\ V\ vs\ SHE$$

$$Fe(OH)_2 = \gamma - FeOOH + H^+ + e^- \quad (10)$$

$$E = 0.187 - 0.059\ pH$$
$$= -0.421\ V\ vs\ SHE$$

$$2[Fe(OH)_2 \cdot 2FeOOH] = 3\gamma - Fe_2O_3 + 2H^+ + 3H_2O + 2e^- \quad (11)$$

$$E = 0.296 - 0.059\ pH$$
$$= -0.312\ V\ vs\ SHE$$

Consideration of the above equilibrium potentials in the light of the polarization curves obtained in this work (Figures 1, 2, 4, 6) reveals that Reactions 4–9 can in principle contribute to the anodic currents measured in the active region, from about −550 mV vs SHE to about −480 mV vs SHE. On the other hand, reactions 10 and 11 take place only under potentials more noble than the peak potential, in the region of passive layer formation, i.e. in the descending part of peak A.

The work of Refait et al. [30] also revealed that green rust carbonate ($Fe_6(OH)_{12}CO_3 \cdot 2\ H_2O$), which has a standard free energy of formation of −966 kJ mol^{-1}, is much more stable than the green rust chloride ($Fe_4(OH)_8Cl \cdot nH_2O$), which has a standard free energy of formation of only −506 kJ mol^{-1}, all at 25 °C. These thermodynamic predictions were borne out when they found that only green rust carbonate (Equation 5) formed upon the corrosion of iron in a medium composed of 0.1 M HCO_3^- + 4.0 M Cl^- and no green rust chloride (Equation 7) was detected [30], despite the fact that the ratio of chloride to bicarbonate concentrations was 40. In view of this evidence, it can be concluded that green rust chloride (Equation 7) does not form under the conditions of the present measurements. Consequently, Equation 7 is excluded from contributing to the currents measured in the active region. This evidence also explains the lack of significant effects of chloride ion on the rate of metal dissolution in the active region and at the free corrosion potential, as shown by both the polarization and impedance measurements.

5. Conclusions

Chloride ions have a strong deleterious effect on the passivity of low carbon steel in carbonate–bicarbonate buffer of (pH 10.3), see Equation 1 and Figure 2, while the passivity of the of the metal improved with increase of the concentration of the carbonate–bicarbonate buffer. Conversely, chloride ions have only a small effect on the rate of iron dissolution at the free corrosion potential and in the active region, as judged by a reaction order of 0.1 (Figure 5). This value is much lower than the values of 0.5 and 1.1 reported in strongly acidic media [43] and hence reveals a different mechanism than that already established for chloride ion in the acid medium. The results of the present measurements in the active region find interpretation in the thermodynamic predictions of Refait et al. [30] which favor the formation of iron carbonate rather than iron chloride complexes.

In the light of the present results, it can be concluded that the injection of alkalis in wells to raise the pH minimizes the effect of chloride ions on the corrosion of iron, in addition to decreasing the acidity of the geothermal brines. However, they point to the dangers of the pitting of iron if the corrosion potential is shifted into the passive region, for example under the effect of oxygen which may be dissolved in these alkalis or in other waters injected in the wells.

Acknowledgement

The authors gratefully acknowledge the Research Administration of Kuwait University (grant SC 104) for their financial support.

Appendix 1

In a potentiodynamic experiment, the magnitude of the charging current, i_c, A cm^{-2} is related to the potential scanning rate, dE/dt, (V s^{-1}) and the double layer capacity of the electrode, C (F cm^{-2}) by

$$i_c = C\, dE/dt \tag{A.1}$$

Taking a nominal value of $C = 25 \times 10^{-6}$ F cm^{-2} and using values of $dE/dt = 0.1$ up to 20 mV s^{-1}, the above equation gives values of i_c of 2.5 nA cm^{-2} and 0.5 μA cm^{-2}, respectively. These values are negligible compared to the measured currents in the passive region in Figure 6.

References

1. L. Garverik (Ed.), Corrosion in Petroleum Production Operations, *in* 'Corrosion in the Petrochemical Industry', (ASM International, Metals Park, OH, 1994), p. 279.
2. L.E. Newton and R.H. Hausler, (Eds), Houston, CO_2 Corrosion in Oil and Gas Production', (NACE, Houstan, TX 1984).
3. Y.J. Tan, S. Bailey, B. Kinsella and A. Lowe, *J. Electrochem. Soc.*, **147** (2000) 530.
4. C. de Waard, U. Lotz and D.E. Milliams, *Corrosion* **47** (1991) 976.
5. Z. Xia, K.C. Chou and Z. Szklarska-Smialowska, *Corros. Sci.* **45** (1989) 636.
6. R.N. Tuttle and R.D. Kane, 'H_2S Corrosion in Oil and Gas Production: A Compilation of Classic Papers' (NACE, Houson, TX 1981).
7. L. Bertolini, F. Bolzani, T. Pastore and P. Pedeferri, *Br. Corr. J.* **31** (1996) 218.
8. G. Nakayama, Y. Fukaya and M. Akashi, *in* 'Electrochemical Synthesis and Modification of Materials', Material Research Society Symposia (MRS) Proceedings, Vol. 451, (MRS, Pittsburg, 1997), p. 567.
9. R.N. Parkins, C.S. O'Dell and R.R. Fessler, *Corros. Sci.* **24** (1984) 34.
10. M. Odziemkowski, J. Flis and D.E. Irish, *Electrochim. Acta* **39** (1994) 2225.
11. J.K. Heuer and J.F. Stubbins, *Corros. Sci.* **41** (1999) 1231.
12. J.M. Blengino, M. Keddam, J.P. Kabbe and L. Robbiola, *Corros. Sci.* **37** (1995) 621.
13. L.J. Simpson and C.A. Melendres, *J. Electrochem, Soc.* **143** (1996) 2146.
14. E.B. Castro, S.G. Real, R.H. Milocco and J.R. Vilche, *Electrchim. Acta* **36** (1991) 117.
15. L.J. Oblonsky and T.M. Devine, *J. Electrochem. Soc.* **144** (1997) 1252.
16. G. Fierro, G.M. Ingo and F. Mancia, *Corrosion* **45** (1989) 814.
17. M. Abdelmoula, Ph. Refait, S.H. Drissi, J.P. Mihe and J.M.R. Genin, *Corros. Sci.* **38** (1996) 623.
18. S.L. Hirnyi, *Mater. Sci.* (Russia) **37** (2001) 87.
19. Y.F. Cheng and J.L. Luo, *J. Electrochem. Soc.* **146** (1999) 970.
20. B.R. Linter and G.T. Burstein, *Corros. Sci.* **41** (1999) 117.

21. E.B. Castro, J.R. Vilche and A.J. Arvia, *Corros. Sci.* **32** (1991) 37.
22. J. O'M Bockris and S.U. Khan, 'Surface Electrochemistry: A Molecular Level Approach' (Plenum Press, New York, 1993), p. 756.
23. W.J. Lorenz and K.E. Heusler, Anodic Dissolution of Iron Group Metals, *in* F. Mansfield (Ed.), 'Corrosion Mechanism', (Marcel Dekker, New York, 1987), p. 1.
24. D.M. Drazic, The electrochemistry of iron in an active state, *in* J.O'M. Bockris and B.E. Conway, (Ed.), 'Modern Aspects of Electrochemistry', Vol. 19, (Plenum Press, New York, 1989), p. 69.
25. M. Keddam, Anodic dissolution, *in* P. Marcus and J. Oudar, (Ed.), 'Corrosion Mechanisms in Theory and Practice', (Marcel Dekker, New York, 1995), p. 55.
26. K.E. Heusler, *in* A.J. Bard (Ed.), 'Encyclopedia of the Electrochemistry of the Elements' Vol. 9A, (Marcel Dekker, New York, 1982), p. 230.
27. Ph. Refait and J.M.R. Genin, *Corros. Sci.* **34** (1993) 797.
28. S.H. Drissi, Ph. Refait, M. Abdelmoula and J.M.R. Genin, *Corros. Sci.* **37** (1995) 2025.
29. J.M.R. Genin, A.A. Olowe, Ph. Refait and L. Simon, *Corros. Sci.* **38** (1996) 1751.
30. Ph. Refait, S.H. Drissi, J. Pytkiewicz and J.M.R. Genin, *Corros. Sci.* **39** (1997) 1710.
31. Ph. Refait, M. Abdelmoula and J.M.R. Genin, *Corros. Sci.* **40** (1998) 1560.
32. J. Stewart, P.H. Balkwill and D.E. Williams, *Corros. Sci.* **36** (1994) 1213.
33. G.S. Frankel, *J. Electrochem Soc.* **45** (1998) 2186.
34. Z. Szklarska-Smialowska, 'Pitting Corrosion of Metals' (NACE, Houston, TX, 1986), p. 204 and 347.
35. D. Sazou, A. Diamantopoulou and M. Pagitsas, *J. Electroanal. Chem.* **499** (2000) 1.
36. L.F. Garfias- Mesias and J.M. Sykes, *Corros. Sci.* **41** (1999) 959.
37. T.T. Lunt, S.T. Pride, J.R. Scully, J.L. Hudson and A.S. Mikhailov, *J. Electrochem. Soc.* **144** (1997) 1620; B. Wu, J.R. Scully, J.L. Hudson and A.S. Mikhailov, *Ibid* **144** (1997) 1614.
38. Y. Zuo, H. Wang, J. Zhao and J. Xiong, *Corros. Sci.* **44** (2002) 13.
39. Y.F. Cheng, M. Wilmott and J.L. Lou, *Br. Corr. J.* **34** (1999) 280.
40. Carmel B. Breslin, Digby D. Macdonald, Janusz Sikora and Elzbieta Sikora, *Electrochim. Acta* **42** (1997) 127.
41. P.C. Pistorius and G.T. Burstein, *Corros. Sci.* **36** (1994) 525; G.T. Burstein, P.C. Pistorius and S.P. Mattin, *Ibid* **35** (1993) 57.
42. G.L.Makar and D. Tromans, *Corrosion* **52** (1996) 250.
43. R.J. Chen and K. Nobe, *J. Electrochem. Soc.* **119** (1972) 1457.
44. A.J. Bard and L.R. Faulkner, 'Electrochemical Methods: Fundamentals and Applications', (Wiley, New York, 1980), p. 218.